THE JOURNAL OF PHYSICAL CHEMISTRY A LETTERS

**2005,** *109,* 9388−9392
Published on Web 10/01/2005

# Physical Properties and Intermolecular Dynamics of an Ionic Liquid Compared with Its Isoelectronic Neutral Binary Solution

**Hideaki Shirota* and Edward W. Castner, Jr.***

*Department of Chemistry and Chemical Biology, Rutgers, The State University of New Jersey, 610 Taylor Road, Piscataway, New Jersey 08854-8087*

*Received: August 18, 2005; In Final Form: September 13, 2005*

In this study, we address the following question about room-temperature ionic liquids (RTILs). Are the properties of a RTIL more dependent on the charges of the molecular ions or on the fact that the liquid is a complex mixture of two species, one or both of which are asymmetric? To address this question and to better understand the interactions and dynamics in RTILs, we have prepared the organic ionic liquid 1-methoxyethylpyridinium dicyanoamide ($MOEPy^+/DCA^-$) and compared this RTIL with the analogous isoelectronic binary solution, comprised of equal parts of 1-methoxyethylbenzene (MOEBz) and dicyanomethane (DCM). In essence, we have created a RTIL and a nearly identical neutral pair in which we have effectively turned off the charges. To understand the intermolecular interactions in both of these liquids, we have characterized the bulk density and shear viscosity. Using femtosecond optical Kerr effect spectroscopy, we have also characterized the intermolecular vibrational dynamics and diffusive reorientation. To verify that the shape, polarizability, and electronic structure of the RTIL ions and the components of the neutral pair are truly quite similar, we have carried out density functional theory calculations on the individual molecular ion and neutral species.

## Introduction

Room-temperature ionic liquids (RTILs) are of great interest for a variety of immediate and future applications.[1−5] Substantial effort has been devoted to developing new RTILs for specialized applications, but much less attention has been given to obtaining a detailed understanding of their physical chemistry.

The fundamental question we attempt to address in this letter is to understand what fraction of ionic liquid properties are accounted for by the dynamical properties of a binary solution of asymmetric, polar, and polarizable species of different sizes and what fraction of these properties arise from the charge interactions between the molecular ions. In this study, we compare the physical properties and intermolecular vibrational and orientational dynamics of the RTIL 1-methoxyethylpyridinium dicyanoamide ($MOEPy^+/DCA^-$) with the properties and dynamics of the analogous isoelectronic (and nearly isostructural) neutral pair 1-methoxyethylbenzene/dicyanomethane (MOEBz/DCM), shown in Chart 1. Details of the orientational relaxation and of the strength of the intermolecular interactions are obtained from analysis of femtosecond optical heterodyne-detected Raman-induced Kerr effect spectroscopy (OHD-RIKES) experiments.[6−11] The results of this analysis are discussed within the context of an understanding of the electronic structure obtained from density functional theory (DFT) calculations for the RTIL cation and anion and for the two components of the neutral pair liquid. Electrostatic properties for the molecular species that are obtained from DFT results

**CHART 1: RTIL ($MOEPy^+/DCA^-$) and Isoelectronic Molecules of the Neutral Binary Solution (MOEBz/DCM)**

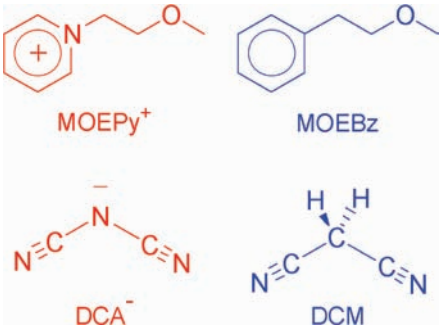


are considered in the context of the measured liquid densities. We compare the measured collective reorientation lifetimes with the shear viscosities to learn that hydrodynamic theories may be relevant for understanding diffusive dynamics in ionic liquids.

## Experimental Section

Femtosecond OHD-RIKES experiments measure the depolarized Raman spectrum as a free induction decay of the birefringence introduced into the optically transparent sample by a femtosecond pump pulse.[6,12] The OHD-RIKES apparatus used here has been described previously.[13,14] All OHD-RIKES measurements were made at 296 ± 2 K. The instrument temporal response, measured with a 200 $\mu$m KDP crystal, was a 40 ± 3 fs full width at half-maximum. Scans with high time resolution of 4096 points at 0.5 $\mu$m/step were recorded for a

* Corresponding authors. E-mail: shirota@rutchem.rutgers.edu (H.S.); castner@rutchem.rutgers.edu. (E.W.C.).

10.1021/jp054664c CCC: $30.25 

**TABLE 1: Formula Weights (fw), van der Waals Volumes ($V$), Viscosities ($\eta$), and Densities ($d$) at 295 K of MOEPy$^+$/DCA$^-$ and MOEBz/DCM**

| liquid | fw[a] (g mol$^{-1}$) | $V^{a,b}$ (Å$^3$) | $\eta^c$ (cP) | $d^d$ (g mL$^{-1}$) |
|---|---|---|---|---|
| MOEPy$^+$/DCA$^-$ | 204.1 (C, 138.1; A, 66.0) | 192.0 (C, 136.6; A, 55.4) | 65.1 | 1.17 |
| MOEBz/DCM | 202.3 (C, 136.2; A, 66.1) | 199.3 (C, 138.0; A, 61.3) | 2.24 | 0.98 |

[a] C and A denote cation and anion. [b] Values are calculated by the sum of van der Waals increments.[22,23] [c] ±5%. [d] ±3%.

time window of 13.66 ps. The slower orientational dynamics were captured in 110 ps scans with 5.0 $\mu$m/step and in 743 ps scans with 50 $\mu$m/step. The Kerr transients measured in the time-domain data are converted to the low-frequency depolarized Raman spectrum by direct Fourier transform deconvolution over the range from 0.02 to >700 cm$^{-1}$.[6,15,16] For the longer 743 ps scans recorded for MOEPy$^+$/DCA$^-$, the 5.0 $\mu$m/step data from −2 to 102 ps were patched with the data from 102 to 743 ps recorded at 50 $\mu$m/step.[17]

The synthesis of MOEPy$^+$/DCA$^-$ is based on standard procedures,[18−20] summarized in the Supporting Information. MOEBz (liquid, TCI) and DCM (solid, Sigma-Aldrich) were used as received and were mixed to obtain a mole fraction of 0.5 for each component. Viscosity measurements were made using a temperature-controlled viscometer (Cambridge Applied Systems, ViscoLab 4100).[17] The MOEPy$^+$/DCA$^-$ ionic liquid was dried for 12 h in a vacuum oven prior to viscosity and OHD-RIKES experiments.

DFT geometry optimization and normal mode calculations for MOEPy$^+$, DCA$^-$, MOEBz, and DCM were performed at the B3LYP/6-311+G(d,p) level of theory using the Gaussian 03 program (revision B.03).[21] The atom-centered charges were obtained using the CHelpG algorithm.

## Results and Discussion

Shear viscosities ($\eta$) and densities ($d$) at 295 K for both MOEPy$^+$/DCA$^-$ and MOEBz/DCM are summarized in Table 1, along with the formula weights and molecular volumes ($V$).[22,23] The volumes for the cation and anion components of the RTIL are slightly smaller than those for the neutral pair by about 4%. However, the density ratio of MOEPy$^+$/DCA$^-$ to MOEBz/DCM is nearly 1.20. We conclude that the packing density is greater in the RTIL than in the neutral binary solution. The viscosity of MOEPy$^+$/DCA$^-$ is about 30 times larger than that of MOEBz/DCM. The increased density and viscosity of the RTIL relative to the neutral pair are both indications that the intermolecular interactions are stronger in the ionic liquid than in the neutral pair liquid. This is not surprising, because the Coulombic and higher order terms to the electrostatic energy for the MOEPy$^+$/DCA$^-$ interactions should cause stronger intermolecular interactions than those for the neutral MOEBz/DCM interaction.

Figure 1 shows the charge distributions for MOEPy$^+$, DCA$^-$, MOEBz, and DCM. The coordinates and charges are summarized in the Supporting Information. The atom-centered charge distribution of MOEPy$^+$ is quite similar to that of MOEBz, but the charge distribution of DCA$^-$ relative to DCM is somewhat different. The cyano group bond dipoles for DCA$^-$ are about twice the value of those for DCM. The physical properties of RTILs such as viscosity, melting point, and density are dramatically affected by anion substitution.[24,25] Likely, this results from a combination of anion sizes, electronic properties, and symmetries relative to the cation.

Figure 2a shows the Kerr transients of MOEPy$^+$/DCA$^-$ and MOEBz/DCM with the short time window, and Figure 2b shows those with the long time window. The MOEPy$^+$/DCA$^-$ Kerr transients are qualitatively similar to those previously reported

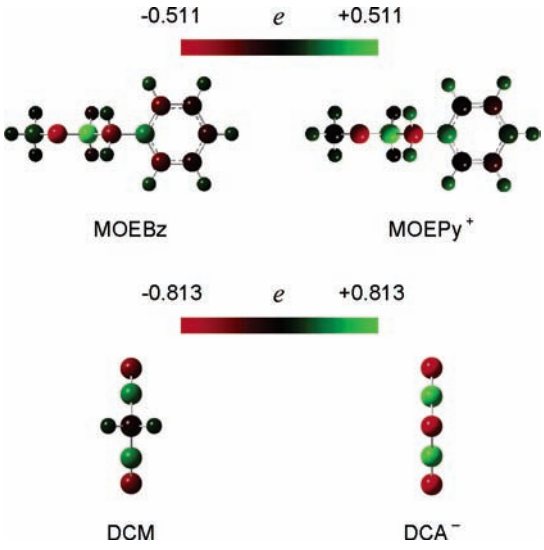


**Figure 1.** Charge distributions of MOEBz, MOEPy$^+$, DCM, and DCA$^-$ at the optimized structure calculated by B3LYP/6-311+G(d,p). The convergence criterion used for the geometry optimization is "tight". The atom-centered charges were obtained using the CHelpG algorithm to fit the electrostatic potential.

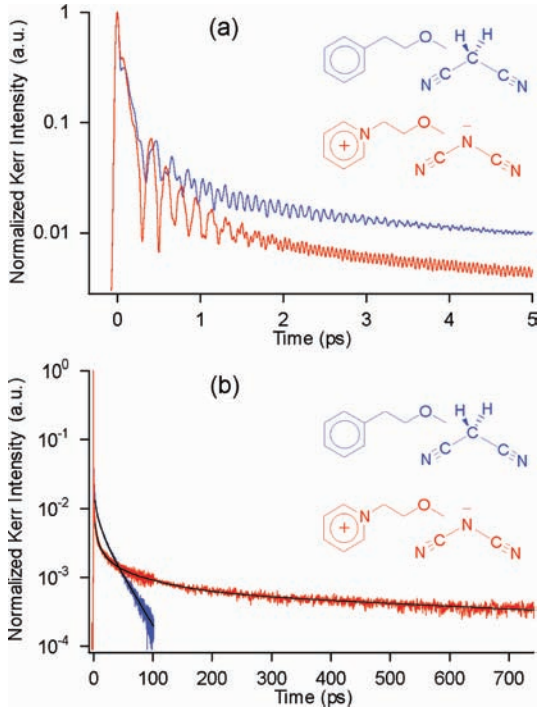


**Figure 2.** OHD-RIKE transients for MOEPy$^+$/DCA$^-$ (red) and MOEBz/DCM (blue): (a) short time window (−0.3 to 5 ps); (b) longer time window (−2 to 740 ps). The fit curves to the orientational relaxation are also shown in part b by black lines.

for imidazolium[17,26−29] and pyrrolidinium ILs.[30] The MOEBz/DCM Kerr transients are in turn qualitatively similar to those reported for neutral aromatic liquids and binary solutions.[31−34] Figure 2b also shows the fit curves to the data (3−743 ps for MOEPy$^+$/DCA$^-$ and 3−101 ps for MOEBz/DCM). A four-

exponential function is used for the $MOEPy^+/DCA^-$ Kerr transient, and a three-exponential function is used for the MOEBz/DCM Kerr transient. Cang, Li, and Fayer showed that the orientational relaxation for the ethylmethylimidazolium nitrate ionic liquid can be best fit to a function comprised of a sum of two power law relaxations multiplied by a longer exponential decay assigned to the α-relaxation.[28] Our $MOEPy^+/DCA^-$ Kerr relaxation data fit nearly as well to the function used by Cang, Li, and Fayer, but we do obtain a slightly better fit to a four-exponential relaxation. The neutral pair liquid data require a sum of three exponential fit functions to obtain the best fit. For the purposes of comparing the two liquids, we have chosen to fit the data to the sum of exponentials for both liquids. The orientational relaxation lifetimes (and the normalized amplitudes) are 2.30 (0.643), 12.20 (0.201), 71.21 (0.103), and 1081 ps (0.053) for $MOEPy^+/DCA^-$ and 1.86 (0.495), 7.58 (0.277), and 29.3 ps (0.228) for MOEBz/DCM. The estimated errors are ±5% for each of the time constants except the longest value of 1081 ps for $MOEPy^+/DCA^-$, which is expected to be substantially larger because the time window extends to only 743 ps, and the amplitude is smallest for this component.

The picosecond reorientation lifetimes for the RTIL and for the neutral molecular mixture are very different, as shown in Figure 2b. $MOEPy^+/DCA^-$ shows a nanosecond relaxation component, while the MOEBz/DCM relaxation is complete in 100 ps. Our previous work on the Kerr spectroscopy of ionic liquids with both pyrrolidinium[30] and silicon-substituted imidazolium[17] cations has shown that the intermediate time constants in the 2−20 ps range do not correlate with viscosity. Because the viscosity ratio between $MOEPy^+/DCA^-$ and MOEBz/DCM is about 30 and the molecular volume ratio between $MOEPy^+/DCA^-$ and MOEBz/DCM is 1.04,[22,23] Stokes−Einstein−Debye (S−E−D) hydrodynamic theory would predict a value of 30.2 for the ratio of the reorientation lifetimes. The ratio between the slowest observed lifetimes $\tau_4(MOEPy^+/DCA^-)/\tau_3$(MOEBz/DCM) is 37, which considering the uncertainty in $\tau_4(MOEPy^+/DCA^-)$ is within the bounds of the estimated errors. Because the constituents of RTILs are molecular ions, the collective reorientation lifetimes obtained from analysis of the Kerr transients are likely to be sensitive to the presence of any clusters, provided that the cluster lifetime exceeds the jump diffusion lifetime. Singly charged cluster signals are observed in the electrospray ionization mass spectrum of $MOEPy^+/DCA^-$, in addition to each of the masses for the constituent anion and cation.[17,35] Thus, we believe that diffusive reorientation for both the $MOEPy^+/DCA^-$ and MOEBz/DCM liquids likely obeys hydrodynamic scaling laws and that the presence of clusters in the RTIL may increase the observed Kerr relaxation lifetime to a value greater than that predicted by S−E−D theory.

As shown in Figure 2a, the Kerr transients of $MOEPy^+/DCA^-$ and MOEBz/DCM contain multiple periodic oscillations arising from the depolarized intramolecular Raman modes. Parts a and b of Figure 3 show the Kerr spectra for $MOEPy^+/DCA^-$ and MOEBz/DCM, respectively, obtained from the transients by Fourier transform deconvolution. The spectra have the contribution from the picosecond relaxation subtracted to emphasize the vibrational dynamics.[17,30] The Kerr spectra are well resolved to >700 $cm^{-1}$. The intramolecular vibrational modes observed in the $MOEPy^+/DCA^-$ and MOEBz/DCM Kerr spectra are assigned on the basis of the DFT calculation results and presented in the Supporting Information. The intense bands at 183 $cm^{-1}$ for $DCA^-$ and 161 $cm^{-1}$ for DCM result from the $NC-N^--CN$ and $NC-CH_2-CN$ bending modes, respectively.

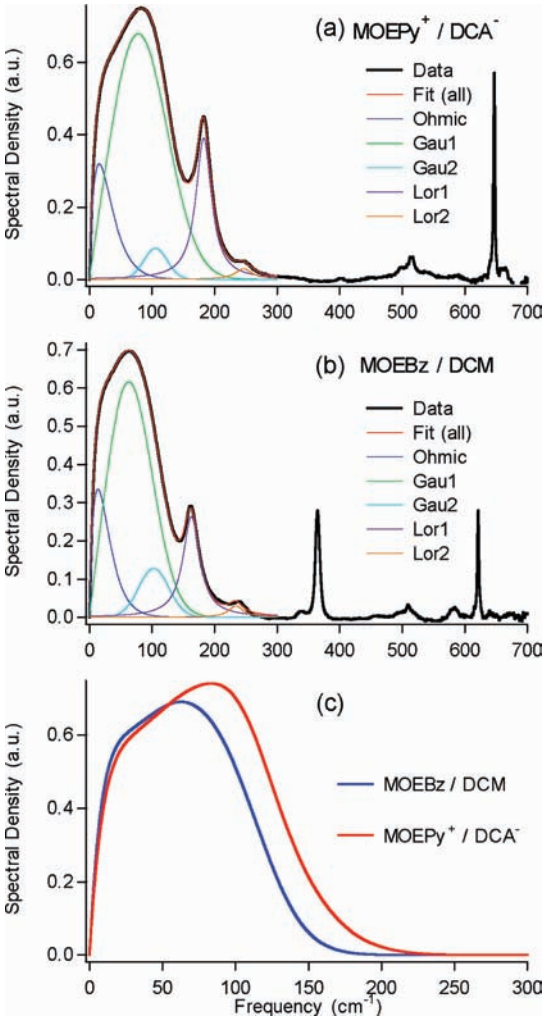


**Figure 3.** OHD-RIKE spectra obtained by Fourier transform deconvolution analysis for (a) $MOEPy^+/DCA^-$ and (b) MOEBz/DCM. (c) Spectral components assigned to intermolecular vibrations, the sum of the Ohmic function plus the two antisymmetrized Gaussian functions, are shown for MOEBz/DCM (blue) and $MOEPy^+/DCA^-$ (red).

The pyridyl ring deformation mode is observed at 647 $cm^{-1}$ for $MOEPy^+$, and the phenyl ring deformation mode is observed at 621 $cm^{-1}$ for MOEBz. The 364 $cm^{-1}$ mode in MOEBz/DCM, absent in $MOEPy^+/DCA^-$, is assigned to the doubly degenerate $CH_2$ rocking and twisting modes.

The broad low-frequency spectrum of a molecular liquid in the 0−250 $cm^{-1}$ frequency range contains contributions that arise from both intramolecular normal modes and intermolecular vibrational motions. The intermolecular dynamics include interaction (dipole−dipole)-induced, collision-induced, and librational motions.[36−40] The inter- and intramolecular dynamics overlap in this spectral region and cannot be distinguished unambiguously, so we attempt to gain further insight into these spectra via line shape analyses. The low-frequency spectra are fit to a composite line shape comprised of the sum of an Ohmic function and two antisymmetrized Gaussian functions, with two Lorentzian functions added to fit the narrower bands assigned to intramolecular normal modes.[17] Figure 3 shows the low-frequency Kerr spectra over the frequency range from 0 to 700 $cm^{-1}$ and the line shape fits over the 0−300 $cm^{-1}$ range, for (a) $MOEPy^+/DCA^-$ and (b) MOEBz/DCM. The fit parameters are summarized in Table 2.

The gas-phase vibrational frequencies obtained from DFT calculations for $MOEPy^+$, $DCA^-$, MOEBz, and DCM are

**TABLE 2: Fit Parameters for the Low-Frequency Kerr Spectra (0−300 cm$^{-1}$) of MOEPy$^+$/DCA$^-$ and MOEBz/DCM**

| Intermolecular Spectral Lineshape Functions | | | | | | | | | |
|---|---|---|---|---|---|---|---|---|---|
| liquid | $M_1$[a] (cm$^{-1}$) | $a_{\mathrm{Ohmic}}$[b,d] | $\omega_{\mathrm{Ohmic}}$[b,e] (cm$^{-1}$) | $a_{G,1}$[c,f] | $\omega_{G,1}$[c,g] (cm$^{-1}$) | $\Delta\omega_{G,1}$[c,h] (cm$^{-1}$) | $a_{G,2}$[c,i] | $\omega_{G,2}$[c,j] (cm$^{-1}$) | $\Delta\omega_{G,2}$[c,k] (cm$^{-1}$) |
| MOEPy$^+$/DCA$^-$ | 78.8 | 0.0554 | 15.7 | 0.682 | 78.0 | 110.0 | 0.086 | 106.0 | 44.2 |
| MOEBz/DCM | 65.9 | 0.0664 | 13.7 | 0.618 | 62.9 | 88.8 | 0.128 | 103.2 | 56.9 |

| Intramolecular Spectral Lineshape Functions | | | | | | |
|---|---|---|---|---|---|---|
| liquid | $a_{L,1}$[l] | $\omega_{L,1}$[l] (cm$^{-1}$) | $\Delta\omega_{L,1}$[l] (cm$^{-1}$) | $a_{L,2}$[l] | $\omega_{L,2}$[l] (cm$^{-1}$) | $\Delta\omega_{L,2}$[l] (cm$^{-1}$) |
| MOEPy$^+$/DCA$^-$ | 18.54[m] | 182.8[m] | 15.1[m] | 1.497[n] | 246.9[n] | 16.4[n] |
| MOEBz/DCM | 13.49[o] | 163.1[o] | 16.3[o] | 1.314[p] | 234.4[p] | 14.1[p] |

[a] $M_1 = \int\omega I(\omega)\,\mathrm{d}\omega/\int I(\omega)\,\mathrm{d}\omega$. [b] $I_{\mathrm{Ohmic}}(\omega) = \alpha_{\mathrm{Ohmic}}\omega\exp(-\omega/\omega_{\mathrm{Ohmic}})$. [c] $I_G(\omega) = \sum_i a_{G,i}\{\exp[2(\omega-\omega_{G,i})^2/(2\ln(2)(\Delta\omega_{G,i})^2)] - \exp[2(\omega-\omega_{G,i})^2/(2\ln(2)(\Delta\omega_{G,i})^2)]\}$. [d] ±5%. [e] ±2%. [f] ±5%. [g] ±3%. [h] ±3%. [i] ±5%. [j] ±3%. [k] ±6%. [l] $I_L(\omega) = (1/\pi)\sum_i a_{L,i}/[(\omega-\omega_{L,i})^2 + (\Delta\omega_{L,i})^2]$. [m] DCA$^-$ (C−N$^-$−C bending). [n] MOEPy$^+$ (MOE−Py$^+$ bending). [o] DCM (C−CH$_2$−C bending). [p] MOEBz (MOE−Ph bending).

tabulated in the Supporting Information. The lowest frequencies for the smaller DCA$^-$ and DCM are the bending modes at 164 and 148 cm$^{-1}$, respectively. The MOEPy$^+$ cation modes are predicted at 36, 66, 80, and 95 cm$^{-1}$, while the MOEBz modes are predicted at 35, 81, 81, and 103 cm$^{-1}$. Though depolarized, the Raman cross sections are predicted to be rather smaller than the DCA$^-$ and DCM bending modes. The Ph−R bending frequencies for alkylbenzenes and halogenated benzenes decrease from 100 to 220 cm$^{-1}$ as the mass of the alkyl or halogen group increases.[34,41] The present DFT calculation results also predict that the bending mode frequencies of MOE−Py$^+$ and MOE−Bz are about 80 cm$^{-1}$. However, clear intramolecular vibrational bands are not observed in the low-frequency Kerr spectra shown in Figure 3 for the frequency range from 0 to 150 cm$^{-1}$. Figure 3c shows the low-frequency Kerr spectral components from the sum of an Ohmic function and two antisymmetrized Gaussian functions in order to focus on the broad *intermolecular* spectral features.

As shown in Figure 3c, the low-frequency Kerr spectrum of MOEPy$^+$/DCA$^-$ has a much broader width and higher frequency peak than that of MOEBz/DCM. The full width at half-maximum values from the broad low-frequency Kerr spectra of MOEPy$^+$/DCA$^-$ and MOEBz/DCM (Figure 3c) are 125.0 and 109.5 cm$^{-1}$, respectively, and the peaks are 82.9 cm$^{-1}$ for MOEPy$^+$/DCA$^-$ and 62.4 cm$^{-1}$ for MOEBz/DCM. Another simple means of comparing the intermolecular vibrational dynamics is via the first moment of the overall spectrum. The first moment ($M_1$) is 78.8 cm$^{-1}$ for MOEPy$^+$/DCA$^-$, which is substantially higher than the value 65.9 cm$^{-1}$ for MOEBz/DCM. Generally, the value of the spectral peak frequency for the low-frequency Kerr spectra of amorphous solids and supercooled liquids is larger than that for molecular liquids.[7] Intermolecular vibrational frequencies have been shown to increase with decreasing temperature for both $CS_2$ and $CH_3CN$; the intermolecular potential steepens concurrently with the density increase.[42] Regardless of how one characterizes the low-frequency spectra for MOEPy$^+$/DCA$^-$ and MOEBz/DCM, it is clear that the center of the intermolecular spectral density is about 20% higher for the ionic liquid compared to the isoelectronic, isostructural neutral pair, for which the mass is reduced by 1%. Thus, we must conclude that the aggregate intermolecular interactions have stronger force constants for the ionic liquid than for the neutral pair. The overall increase in force constants for MOEPy$^+$/DCA$^-$ relative to MOEBz/DCM is consistent with the fact that the measured density and viscosity values are higher for the ionic liquid than for the neutral binary solution. The MOEPy$^+$/DCA$^-$ RTIL has the additional Coulombic and higher order terms in the electrostatic interaction energy that are not present for the MOEBz/DCM neutral pair. It seems likely that dielectric friction[43] may also be contributing to the increased viscosity in the RTIL relative to the neutral binary solution.

In conclusion, we have created a binary neutral solution to mimic the shape, charge distribution, and mass of an analogous isoelectronic ionic liquid, so as to have a model for the ionic liquid with the net charges on the molecular ions effectively turned off. The densities, viscosities, and intermolecular vibrational frequencies are all higher for MOEPy$^+$/DCA$^-$ than for MOEBz/DCM, indicating stronger interactions for the ionic liquid than for the neutral pair. The slowest lifetimes obtained from analysis of the OHD-RIKES transients are 1.08 ns for MOEPy$^+$/DCA$^-$ and 29 ps for MOEBz/DCM. The ratio of these reorientational lifetimes scales with the ratio of the measured viscosity values, indicating that hydrodynamic scaling theories may be relevant for describing orientational friction. Many promising experimental opportunities are available to compare the ionic liquid and the isoelectronic neutral binary solutions to further elucidate the structural, dynamical, and thermodynamic properties of RTILs. Continuing work on this system includes temperature dependent OHD-RIKES, NMR, and time-resolved fluorescence probe studies.

**Acknowledgment.** We gratefully acknowledge funding support from the National Science Foundation (CHE-0239390) and the donors of the ACS Petroleum Research Fund (42375-AC6). We thank Dr. James F. Wishart (Brookhaven National Laboratory) and Prof. Mark N. Kobrak (Brooklyn College) for stimulating discussions.

**Supporting Information Available:** Details of the synthesis and characterization of MOEPy$^+$/DCA$^-$ and MOEBz/DCM are presented. Results from the electronic structure calculations are tabulated for each of the four molecular species, including atomic coordinates, atom-centered charges, and vibrational frequencies. This material is available free of charge via the Internet at http://pubs.acs.org.

## References and Notes

(1) *Ionic Liquids IIIA: Fundamentals, Progress, Challenges, and Opportunities. Properties and Structure*; Rogers, R. D., Seddon, K. R., Eds.; ACS Symposium Series 901; American Chemical Society: Washington, DC, 2005.

(2) *Ionic Liquids IIIB: Fundamentals, Progress, Challenges, and Opportunities. Transformation and Processes*; Rogers, R. D., Seddon, K. R., Eds.; ACS Symposium Series 902; American Chemical Society: Washington, DC, 2005.

(3) Welton, T. *Chem. Rev.* **1999**, *99*, 2071.

(4) Wasserscheid, P.; Keim, W. *Angew. Chem., Int. Ed.* **2000**, *39*, 3772.

(5) Earle, M. J.; Seddon, K. R. *Pure Appl. Chem.* **2000**, *72*, 1398.

(6) Lotshaw, W. T.; McMorrow, D.; Thantu, N.; Melinger, J. S.; Kitchenham, R. *J. Raman Spectrosc.* **1995**, *26*, 571.

(7) Kinoshita, S.; Kai, Y.; Ariyoshi, T.; Shimada, Y. *Int. J. Mod. Phys. B* **1996**, *10*, 1229.

(8) Castner, E. W., Jr.; Maroncelli, M. *J. Mol. Liq.* **1998**, *77*, 1.

(9) Smith, N. A.; Meech, S. R. *Int. Rev. Phys. Chem.* **2002**, *21*, 75.

(10) Loughnane, B. J.; Farrer, R. A.; Scodinu, A.; Reilly, T.; Fourkas, J. T. *J. Phys. Chem. B* **2000**, *104*, 5421.
(11) Farrer, R. A.; Fourkas, J. T. *Acc. Chem. Res.* **2003**, *36*, 605.
(12) McMorrow, D.; Lotshaw, W. T.; Kenney-Wallace, G. A. *IEEE J. Quantum Electron.* **1988**, *24*, 443.
(13) Shirota, H.; Castner, E. W., Jr. *J. Am. Chem. Soc.* **2001**, *123*, 12877.
(14) Wiewior, P. P.; Shirota, H.; Castner, E. W., Jr. *J. Chem. Phys.* **2002**, *116*, 4643.
(15) McMorrow, D.; Lotshaw, W. T. *Chem. Phys. Lett.* **1990**, *174*, 85.
(16) McMorrow, D.; Lotshaw, W. T. *J. Phys. Chem.* **1991**, *95*, 10395.
(17) Shirota, H.; Castner, E. W., Jr. *J. Phys. Chem. B*, in press.
(18) Katritzky, A. R.; Watson, C. H.; Dega-Szafran, Z.; Eyler, J. R. *J. Am. Chem. Soc.* **1990**, *112*, 2471.
(19) Noda, A.; Watanabe, M. *Electrochim. Acta* **2000**, *45*, 1265.
(20) MacFarlane, D. R.; Forsyth, S. A.; Golding, J.; Deacon, G. B. *Green Chem.* **2002**, *4*, 444.
(21) Frisch, M. J.; Trucks, G. W.; Schlegel, H. B.; Scuseria, G. E.; Robb, M. A.; Cheeseman, J. R.; Montgomery, J. A., Jr.; Vreven, T.; Kudin, K. N.; Burant, J. C.; Millam, J. M.; Iyengar, S. S.; Tomasi, J.; Barone, V.; Mennucci, B.; Cossi, M.; Scalmani, G.; Rega, N.; Petersson, G. A.; Nakatsuji, H.; Hada, M.; Ehara, M.; Toyota, K.; Fukuda, R.; Hasegawa, J.; Ishida, M.; Nakajima, T.; Honda, Y.; Kitao, O.; Nakai, H.; Klene, M.; Li, X.; Knox, J. E.; Hratchian, H. P.; Cross, J. B.; Adamo, C.; Jaramillo, J.; Gomperts, R.; Stratmann, R. E.; Yazyev, O.; Austin, A. J.; Cammi, R.; Pomelli, C.; Ochterski, J. W.; Ayala, P. Y.; Morokuma, K.; Voth, G. A.; Salvador, P.; Dannenberg, J. J.; Zakrzewski, V. G.; Dapprich, S.; Daniels, A. D.; Strain, M. C.; Farkas, O.; Malick, D. K.; Rabuck, A. D.; Raghavachari, K.; Foresman, J. B.; Ortiz, J. V.; Cui, Q.; Baboul, A. G.; Clifford, S.; Cioslowski, J.; Stefanov, B. B.; Liu, G.; Liashenko, A.; Piskorz, P.; Komaromi, I.; Martin, R. L.; Fox, D. J.; Keith, T.; Al-Laham, M. A.; Peng, C. Y.; Nanayakkara, A.; Challacombe, M.; Gill, P. M. W.; Johnson, B.; Chen, W.; Wong, M. W.; Gonzalez, C.; Pople, J. A. *Gaussian 03*; Gaussian, Inc.: Pittsburgh, PA, 2003.
(22) Edwards, J. T. *J. Chem. Educ.* **1970**, *47*, 261.
(23) Bondi, A. *J. Phys. Chem.* **1964**, *68*, 441.
(24) Willkes, J. S.; Zaworotko, M. J. *J. Chem. Soc., Chem. Commun.* **1992**, 965.
(25) Bonhote, P.; Sias, A.-P.; Papageorgiou, N.; Kalyanasundaram, K.; Gratzel, M. *Inorg. Chem.* **1996**, *35*, 1168.
(26) Hyun, B. R.; Dzyuba, S. V.; Bartsch, R. A.; Quitevis, E. L. *J. Phys. Chem. A* **2002**, *106*, 7579.
(27) Rajian, J. R.; Li, S.; Bartsch, R. A.; Quitevis, E. L. *Chem. Phys. Lett.* **2004**, *393*, 372.
(28) Cang, H.; Li, J.; Fayer, M. D. *J. Chem. Phys.* **2003**, *119*, 13017.
(29) Giraud, G.; Gordon, C. M.; Dunkin, I. R.; Wynne, K. *J. Chem. Phys.* **2003**, *119*, 464.
(30) Shirota, H.; Funston, A. M.; Wishart, J. F.; Castner, E. W., Jr. *J. Chem. Phys.* **2005**, *122*, 184512.
(31) Neelakandan, M.; Pant, D.; Quitevis, E. L. *Chem. Phys. Lett.* **1997**, *265*, 283.
(32) Ricci, M.; Bartolini, P.; Chelli, R.; Cardini, G.; Califano, S.; Righini, R. *Phys. Chem. Chem. Phys.* **2001**, *3*, 2795.
(33) Smith, N. A.; Meech, S. R. *J. Phys. Chem. A* **2000**, *104*, 4223.
(34) Shirota, H. *J. Chem. Phys.* **2005**, *122*, 044514.
(35) Zhao, D. *Aust. J. Chem.* **2004**, *57*, 509.
(36) Madden, P. A.; Cox, T. I. *Mol. Phys.* **1981**, *43*, 287.
(37) Madden, P. A. In *Molecular Liquids: Dynamics and Interactions*; Yarwood, J., Ed.; D. Reidel Publishing Company: Dordrecht, The Netherlands, 1984; p 431.
(38) Geiger, L. C.; Ladanyi, B. M. *J. Chem. Phys.* **1988**, *89*, 6588.
(39) Geiger, L. C.; Ladanyi, B. M. *Chem. Phys. Lett.* **1989**, *159*, 413.
(40) Ryu, S.; Stratt, R. M. *J. Phys. Chem. B* **2004**, *108*, 6782.
(41) Beard, M. C.; Lotshaw, W. T.; Korter, T. M.; Heilweil, E. J.; McMorrow, D. *J. Phys. Chem. A* **2004**, *108*, 9348.
(42) Farrer, R. A.; Loughnane, B. J.; Deschenes, L. A.; Fourkas, J. T. *J. Chem. Phys.* **1997**, *106*, 6901.
(43) Horng, M. L.; Gardecki, J. A.; Maroncelli, M. *J. Phys. Chem. A* **1997**, *101*, 1030.